Available online at www.sciencedirect.com
SCIENCE DIRECT
Polymer 46 (2005) 2086–2096
polymer
www.elsevier.com/locate/polymer

Polymeric dispersions of model azobenzene dyes

Angelina Altomare, Francesco Ciardelli, Maja Marchini, Roberto Solaro*

University of Pisa, Department of Chemistry and Industrial Chemistry, via Risorgimento 35, 56126 Pisa, Italy

Received 9 September 2004; received in revised form 6 December 2004; accepted 15 December 2004
Available online 28 January 2005

Abstract

New host–guest systems were prepared by using poly(vinyl acetate) and different ethylene–vinyl acetate copolymers as polymeric hosts because of their good compatibility with polar molecules. Two symmetric azobenzene diesters, that is 4,4′-dicarboxyethylazobenzene and 4,4′-di(2-ethylhexyloxycarbonyl)azobenzene were selected as guests. Both solution casting and melt processing were adopted for the preparation of dispersion films that were thoroughly characterized by thermal analysis, UV–vis and FT-IR spectroscopy, and by polarized optical microscopy. The reported results indicate that solution casting afforded heterogeneous dispersions of dye microcrystals at guest concentrations larger than 0.3% whereas homogeneous colored films were obtained at lower dye contents. On the other hand, both melt processing and the presence of branched diester groups favored the dye dispersion within the polymer matrix. At 0.1% dye content, the adopted preparation technique did not appreciably affect the film properties. After 4–8 fold stretching, the host–guest films were analyzed by polarized light spectroscopy. Some of the investigated films displayed interesting polarization efficiency, potentially suited for the preparation of thin film polarizers.

Keywords: Host–guest systems; Azobenzene containing polymers; Optical polarizers

1. Introduction

The need for materials better suited for the emerging technological applications has prompted the study of new polymers. In this respect, the preparation of systems containing azobenzene moieties appears to be very promising. Indeed, the photoinduced *trans–cis* isomerization of azobenzene chromophores can give rise to photochromic and optical dichroic effects [1]. These properties are attracting increasing attention because of their potential industrial applications [2]. Azobenzene containing polymers have been investigated for the preparation of holographic optical memories [3–5], the photo-controlled release of drugs [6], the preparation of polymeric dyes [7–9], and non-linear optical materials [10–13].

The widespread use of liquid crystal displays also promoted the search for low-cost polarizer with improved properties. This goal can be reached either by the design of new materials or by blending existing polymers with suitable additives. In particular, the optical, photoconducting, and photorefractive properties of host–guest polymeric systems containing dispersed azobenzene derivatives were investigated [14–18]. However, homogeneous blends can be obtained only when the dispersed component positively interacts with the polymer matrix, otherwise phase-separated mixtures are obtained. Of course, the blending technique can dramatically affect the mixing kinetics and hence the final morphology of the host–guest system.

Since many years, our interest has been aimed at the preparation of polymeric materials containing photochromic azobenzene chromophores [19–26]. In the present paper, we report the results of an investigation on the synthesis and characterization of azobenzene host–guest systems potentially useful for the fabrication of optical polarizers as well as of food-packaging materials.

2. Experimental

2.1. Materials and instrumentation

2.1.1. Reagents

Reagent grade (Aldrich) 2-ethyl-1-hexanol, ethylene

* Corresponding author. Tel.: +39 050 2219284; fax: +39 050 28438.
E-mail address: rosola@dcci.unipi.it (R. Solaro).

0032-3861/$ - see front matter © 2005 Elsevier Ltd. All rights reserved.
doi:10.1016/j.polymer.2004.12.051

glycol, and dimethyl terephthalate were distilled under vacuum. All other commercial reagents (Aldrich) were used as received.

2.1.2. Polymers

Poly(vinyl acetate) (PVAc, MW 140 kDa) and poly (ethylene-*co*-vinyl acetate) samples containing 40 (EVAc40, Aldrich), 25 (EVAc25, Aldrich), 14 (EVAc14, Greenflex), and 9 wt% (EVAc9, Greenflex) of vinyl acetate units were used as received.

2.1.3. Product characterization

FT-IR spectra were recorded on sample films or KBr pellets by a 1640 Perkin–Elmer spectrophotometer. Microscopy ATR FT-IR spectra were recorded by Perkin Elmer mod. GX spectrometer connected to a Perkin–Elmer Autoimage system. ^{1}H NMR spectra were recorded at 200 MHz on 5–10% sample solutions in perdeuterated solvents with a Varian Gemini 200 spectrometer, by using the following experimental conditions: 11,968 data points, 3 kHz spectral width, 30° pulse, 2 s acquisition time, 1 transient. UV–vis spectra were recorded between 250 and 700 nm at 25 °C in 1 cm quartz cells with a Jasco 7850 spectrophotometer. Polarized light UV–vis measurements were performed by using a Jasco 7850 spectrometer equipped with Sterling Optics polarizer deposited on quartz; polymer films were soaked in high purity silicon oil and placed between two quartz slides. Size exclusion chromatography (SEC) analyses were carried out in chloroform with a 600E Waters liquid chromatograph equipped with two PL Mixed C 5 μm columns, 486 Waters UV detector, and 410 Waters RI detector, by using polystyrene standards for calibration. Thermal gravimetric analyses (TGA) were carried out under nitrogen atmosphere in the 25–600 °C range at 10 °C/min scanning rate on 10–20 mg samples by a Mettler TG 50 instrument. Differential scanning calorimetry (DSC) measurements were performed under nitrogen atmosphere between 0 and 400 °C at 10–20 °C/min on 5–10 mg samples by Mettler DSC 30 calorimeter. Glass transition temperatures were measured from the inflection point in the second heating cycle thermograms; melting enthalpies were evaluated from the integrated areas of melting peaks by using indium for calibration. Melting point determinations and microscopy observations were performed by a Reichert–Jung Polyvar microscope equipped with Mettler FP52 hot plate. Melt processing of polymer–dye mixture was performed with an OHG47055 Brabender mechanical mixer equipped with 30 ml mixing chamber. Compression molding of polymer films was carried out by using a Campana PM20/200 hot press. Film thickness was measured by a Starrett 230 MRL centesimal micrometer. Cast and hot-pressed films were drawn by using a home made hot shoe heated at 40 °C.

2.2. Synthesis of azobenzene dyes

2.2.1. Synthesis of trans-4,4′-dicarboxyazobenzene (DCAAz)

A solution of 13.1 g (78.3 mmol) 4-nitrobenzoic acid and 50.1 g (1.25 mol) NaOH in 225 ml water was heated at 50 °C, then a hot solution of 100.4 g (0.56 mol) α-D-glucose in 150 ml water was added under stirring over 1 h. The stirring was continued for 2 h at 50 °C and overnight at room temperature, then air was bubbled within the resulting solution for 12 h. After addition of acetic acid to pH 6, the solid precipitate was filtered and dried to constant weight to give 9.5 g (90%) of a brownish solid.

FT-IR (KBr pellet): 3300–2500 (ν COOH), 3100–3000 (ν aromatic C–H), 1686 (ν C=O), 1604, 1581 (ν aromatic C=C), 1424 (δ O–H), 1293 (ν C–O), 871 cm^{-1} (δ aromatic C–H). TGA: 1% weight loss at 300 °C, 63.5% weight loss at 460 °C, 31.7 wt% residue at 590 °C. DSC: no endothermal transitions between 25 and 400 °C.

2.2.2. Synthesis of trans-4,4′-dicarboxyethylazobenzene (DEAz)

A solution of 13.7 g (50.6 mmol) DCAAz, 650 ml absolute ethanol, and 16.2 ml 96% sulfuric acid was heated at reflux for 24 h. After cooling at room temperature, the solid precipitate was filtered, suspended in chloroform, and the resulting suspension was washed with water, 5% $NaHCO_3$, and water to neutrality. The suspension was filtered and the organic phase was dried over anhydrous sodium sulfate. After removal of the solvent, the residue was crystallized from 95% ethanol to give 2.44 g (50%) of bright orange crystals having m. p. 144 °C (lit. 143 °C [27]).

FT-IR (KBr pellet): 3100–3000 (ν aromatic C–H), 3000–2850 (ν aliphatic C–H), 1718 (ν C=O), 1600, 1409 (ν aromatic C=C), 1460 and 1370 (δ aliphatic C–H), 1270–1050 (ν C–O–C), 870, 779, 699 cm^{-1} (δ aromatic C–H). ^{1}H-NMR (200 MHz, $CDCl_3$, ppm) $\delta = 8.65$ (d, 4H, aromatic CH *ortho* to the ester group), 8.4 (d, 4H, aromatic CH *ortho* to N=N group), 4.8 (q, 4H, OCH_2), 1.8 (t, 6H, CH_3). UV ($CHCl_3$): λ_{max} (ε) = 330 nm (30,600 l mol^{-1} cm^{-1}) and 460 nm (695 l mol^{-1} cm^{-1}). 1% weight loss at 300°C, 63.5% weight loss at 460°C, 31.7 wt-% residue at 590 °C. DSC: endothermal peak at 144.2 °C.

2.2.3. Synthesis of trans-4,4′-dicarboxyazobenzene dichloride (ClAz)

A suspension of 6.08 g (22.5 mmol) DCAAz in 100 ml thionyl chloride was heated at reflux for 24 h. After removal of volatile products under vacuum, the crude solid was crystallized from *n*-heptane to give 2.2 g (28%) of red crystals. FT-IR (KBr pellet): 3100–3000 (ν aromatic CH), 1778 (ν C=O), 1595, 1577, 1404 (δ aromatic C=C), 885, 861, 804 cm^{-1} (δ aromatic C–H).

Table 1
Preparation of polymer–dye films by solution casting

Sample	Polymer		Azo dye	
	Type	(g)	Type	(g)
SPV	PVAc	1.03	–	–
sPVe1	PVAc	1.01	DEAz	0.011
sPVe2	PVAc	1.15	DEAz	0.023
sPVe3	PVAc	1.05	DEAz	0.033
sPVe01	PVAc	0.90	DEAz	0.001
sPVe02	PVAc	0.90	DEAz	0.002
sPVe03	PVAc	0.91	DEAz	0.003
sPVh01	PVAc	0.90	DHAz	0.001
sPVh02	PVAc	0.89	DHAz	0.002
sPVh03	PVAc	0.93	DHAz	0.003
sE40	EVAc40	1.03	–	–
sE40e1	EVAc40	1.06	DEAz	0.011
sE40e2	EVAc40	1.07	DEAz	0.022
sE40e3	EVAc40	1.09	DEAz	0.032
sE40e01	EVAc40	0.91	DEAz	0.001
sE40e02	EVAc40	0.93	DEAz	0.002
sE40e03	EVAc40	0.91	DEAz	0.004
sE40h01	EVAc40	0.90	DHAz	0.001
sE40h02	EVAc40	0.94	DHAz	0.002
sE40h03	EVAc40	0.79	DHAz	0.002
sE25	EVAc25	1.11	–	–
sE25e1	EVAc25	0.78	DEAz	0.008
sE25e2	EVAc25	0.81	DEAz	0.016
sE25e3	EVAc25	0.80	DEAz	0.024
sE25e01	EVAc25	0.92	DEAz	0.001
sE25e02	EVAc25	0.81	DEAz	0.002
sE25e03	EVAc25	0.71	DEAz	0.002
sE25h01	EVAc25	0.89	DHAz	0.001
sE25h02	EVAc25	0.89	DHAz	0.002
sE25h03	EVAc25	0.91	DHAz	0.003

2.2.4. Synthesis of trans-4,4′-di(2-ethylhexyloxycarbonyl)azobenzene (DHAz)

A suspension of 2.13 g (6.09 mmol) ClAz in 30 ml 2-ethyl-1-hexanol was heated at reflux for 24 h under dry argon atmosphere. After, cooling at room temperature and removal of volatile products under vacuum, the crude solid was eluted over silica gel with 1:1 chloroform/*n*-hexane. The purified product was crystallized from ethanol-water to give 2.6 g (88%) of dark red crystals having m. p. 31–32 °C.

FT-IR (KBr pellet): 3065 (ν aromatic C–H), 2960–2860 (ν aliphatic C–H), 1709 (ν C=O), 1602, 1579 (ν aromatic C=C) 1458, 1411, 1382 (δ aliphatic C–H), 1273–1100

Table 2
Preparation of polymer–dye films by compression molding

Sample	Polymer		Azo dye		Product (g)
	Type	(g)	Type	(g)	
MPV	PVAc	20.83	–	–	19.03
mPVe01	PVAc	20.28	DEAz	0.02	18.95
mPVh01	PVAc	20.78	DHAz	0.02	19.31
mE40	EVAc40	20.19	–	–	14.57
mE40e01	EVAc40	20.35	DEAz	0.02	17.06
mE40h01	EVAc40	20.22	DHAz	0.02	16.05
mE25	EVAc25	20.30	–	–	16.83
mE25e01	EVAc25	20.74	DEAz	0.02	17.73
mE25h01	EVAc25	21.07	DHAz	0.02	16.24
mE14	EVAc14	20.72	–	–	18.32
mE14e01	EVAc14	20.56	DEAz	0.02	19.56
mE14h01	EVAc14	21.12	DHAz	0.02	21.58
mE09	EVAc9	21.36	–	–	18.36
mE09e01	EVAc9	22.53	DEAz	0.02	18.87
mE09h01	EVAc9	20.63	DHAz	0.02	18.99

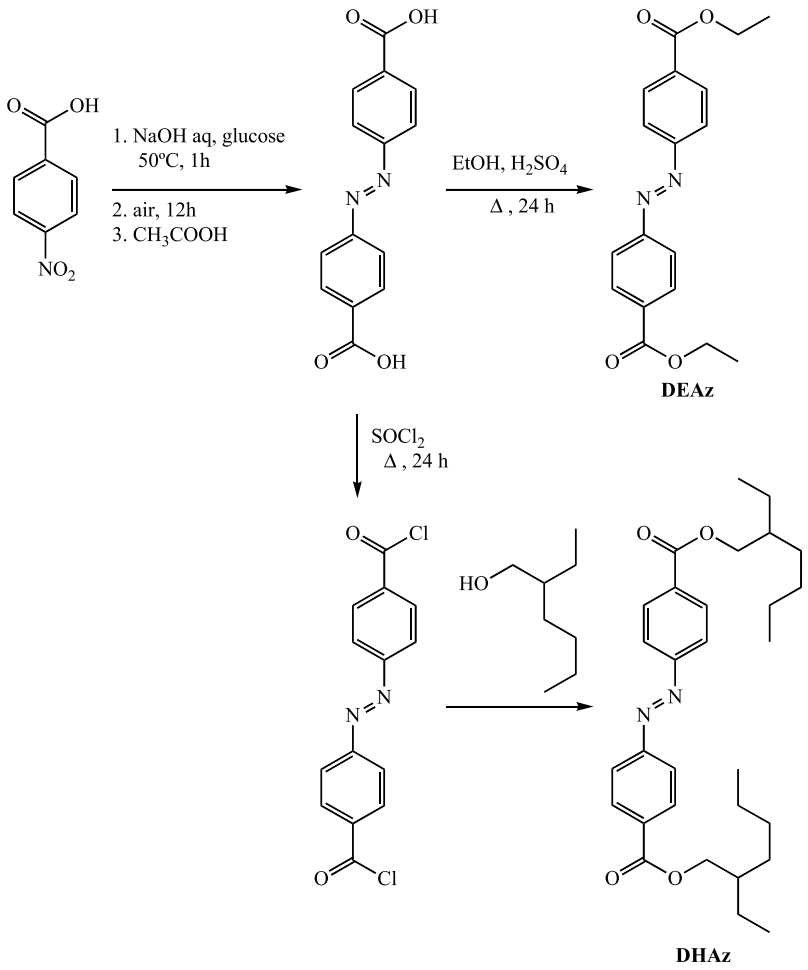

Scheme 1. Reaction sequence adopted for the synthesis of DEAz and DHAz.

(ν C–O–C), 871, 781, 702 cm^{-1} (δ aromatic C–H). ^{1}H-NMR (200 MHz, $CDCl_3$, ppm): $\delta = 8.16$ (d, 4H, aromatic CH *ortho* to ester group), 7.99 (d, 4H, aromatic CH *ortho* to N=N group), 4.28 (q, 4H, CH_2O), 1.74 (m, 2H, CH), 1.35 (m, 12H, CH_2), 0.95 (t, 12H, CH_3). UV ($CHCl_3$): λ_{max} (ε) = 330 nm (33,900 l mol^{-1} cm^{-1}) and 461 nm (730 l mol^{-1} cm^{-1}). TGA: 99.8% weight loss at 392°C, 0.2 residue at 590 °C. DSC: endothermic peak at 32.7 °C.

2.3. Preparation of polymer films

Polymer films were prepared by either solution casting or compression molding, according to general procedures. Data relevant to individual runs are collected in Tables 1 and 2, whereas two typical procedures are described by following.

2.3.1. By solution casting

A suspension of 0.2 g DEAz in 20 ml chloroform was kept under stirring at room temperature for 24 h, then the resulting solution was poured in a 10 cm diameter Petri disk and the solvent was left to evaporate at room temperature for 20 h.

2.3.2. By compression molding

EVAc40 (20 g) and 0.2 g DHAz were mixed in Brabender at 155 °C and 50 rpm for 15 min, then 1.0 g of the resulting material was compressed for 10 min at 160 °C and 25 MPa.

3. Results and discussion

3.1. Synthesis of dyes

The major problem faced with the preparation of host–guest polymer–dye systems is represented by the dye tendency to phase separate with formation of dye aggregates. Therefore, the choice of the dyes was dictated by the need for good compatibility with the host polymers. In this perspective, *trans*-4,4′-dicarboxyazobenzene acid (DCAAz) was selected not only for the ease of synthesis of both low and high molecular weight ester and amide derivatives, but also by taking into account the possibility of interacting with different polymeric matrices by hydrogen bonds, dipole–dipole and van der Waals interactions, and even covalent linkages.

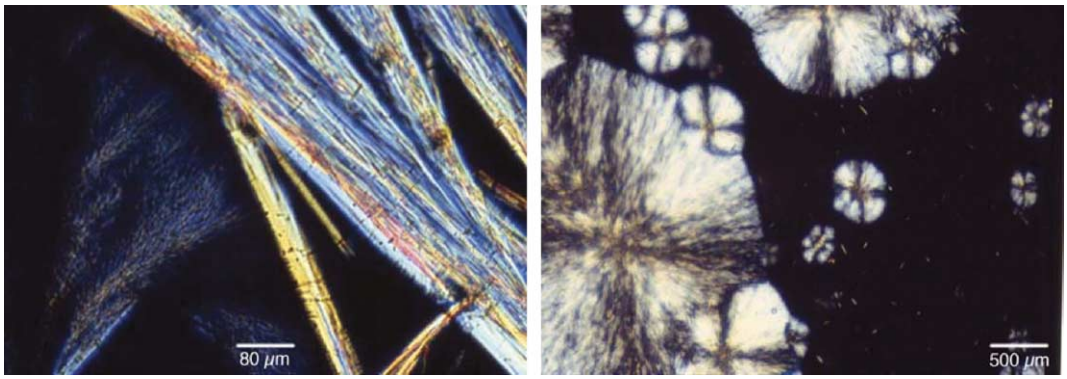

Fig. 1. Polarized optical microscopy images of different regions of PVAc films containing 3% DEAz.

Trans-4,4′-dicarboxyazobenzene (DCAAz) was prepared in 90% yield by glucose reduction of 4-nitrobenzoic acid followed by air oxidation (Scheme 1) [27,28]. Due to its insolubility in common solvents, DCAAz was purified by crystallization of its potassium salt. However, DCAAz cannot be used for the preparation of polymer–dye guest–host systems either by solution casting, because of its very low solubility, or by mixing in the melt. Indeed, DCAAz decomposes before melting. Accordingly, the corresponding diethyl ester, *trans*-4,4′-dicarboxyethylazobenzene (DEAz) was prepared in 50% yield by reaction with ethanol in the presence of sulfuric acid as catalyst.

The presence of long ester alkyl chains can improve the dye affinity and hence miscibility with polyethylene matrices, although long polymethylene chains can promote the dye self-organization and hence phase separation [29]. On the other hand, branched chains of intermediate length should favor dye–polymer interactions while limiting the dye tendency to crystallization. Accordingly, *trans*-4,4′-di(2-ethylhexyloxycarbonyl)azobenzene (DHAz) was prepared in 88% yield by reaction of 4,4′-dicarboxyazobenzene diacid dichloride with 2-ethyl-1-hexanol.

The UV–vis spectrum of the synthesized dyes exhibited two absorption bands at about 330 ($\varepsilon \sim 32{,}000\ \mathrm{l\ mol^{-1}\ cm^{-1}}$) and 450 nm ($\varepsilon \sim 700\ \mathrm{l\ mol^{-1}\ cm^{-1}}$), attributable to azobenzene $\pi \rightarrow \pi^*$ and $n \rightarrow \pi^*$ electronic transitions [30].

3.2. Polymer–dye host–guest systems

Poly(vinyl acetate) (PVAc) and ethylene-vinyl acetate copolymers containing 9 (EVAc9), 14 (EVAc14), 25 (EVAc25), and 40% (EVAc40) of vinyl acetate (VAc) were selected for the preparation of host–guest systems. Indeed, the selected materials join excellent filmability and moderate polarity that should improve the compatibility with polar dyes. Host–guest systems were prepared by casting of chloroform solutions of polymer–dye mixtures. According to this procedure, 50–150 μm films containing 0.1–3% dye were obtained. Films (15–60 μm thickness) were prepared also by melt processing of polymer–dye mixtures at 155 °C followed by molding at 160 °C. In all cases, FT-IR microscopy analysis of the films showed the presence of bands attributable to both the polymeric matrix and the azo dye, although their relative peak intensity changed from site to site.

The compatibility of the prepared polymer–dye mixtures was evaluated by polarized optical microscopy (POM), ATR FT-IR spectroscopy, and by differential scanning calorimetry (DSC). POM analysis was performed on DEAz and DHAz mixtures with PVAc and EVAc containing either 25–40% (cast films) or 9–40% (melt processed films) VAc units. Needle-shaped orange crystals of 4,4′-dicarboxyethylazobenzene and spherulite-like

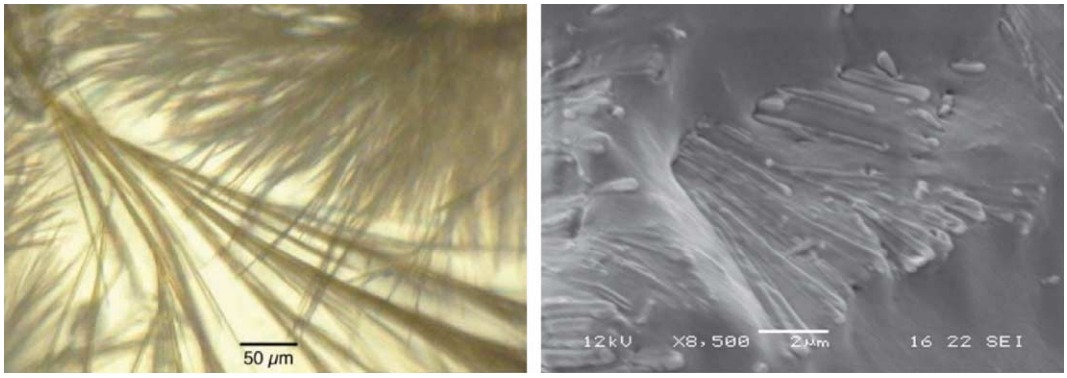

Fig. 2. Optical microscopy image of EVAc40 cast film containing 3% DEAz (left) and SEM micrograph of the film fracture (right).

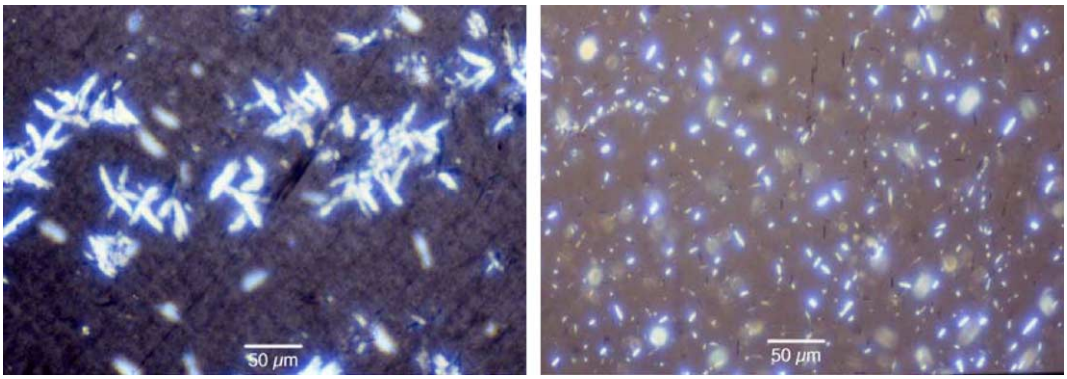

Fig. 3. Polarized optical microscopy images of EVAc40 film containing 1.0 (left) and 0.3% (right) DEAz.

structures were detected in cast films containing 1–3% DEAz (Fig. 1). The latter morphology was much coarser in the case of PVAc films and spherulite-like structures were more abundant at the air interface. POM inspection at higher magnification revealed that each spherulite-like structure was constituted by dendritic clusters of highly branched, needle-like dye crystals originating from a common nucleation center. SEM analysis of the film fracture (Fig. 2) confirmed this indication. The size and the amount of crystalline structures decreased on decreasing the DEAz content, although tiny dye crystals were still detectable at DEAz content as low as 0.3% (Fig. 3). On the other hand, cast films containing either 0.1–0.2% DEAz or 0.1–0.3% DHAz appeared completely homogeneous at optical microscopy observation.

In order to avoid dye crystallization, melt-processed films were prepared by using 0.1% dye. PVAc and EVAc samples containing 9–40% VAc were used as host polymers. None of the melt processed films showed the presence of spherulite-like structures. Moreover, no dye crystal was detected in host–guest systems based on polymers with VAc content larger than 14% and in DHAz-containing films. On the other hand, DEAz mixtures with EVAc9 and EVAc14 presented an almost homogeneous distribution of very small needle-shaped crystals. This behavior confirms that the polymer matrix polarity significantly affects the dye–polymer compatibility.

It is worth noting that no dye crystal was detected when cast films were heated above the dye melting temperature and then cooled down to room temperature, independent of cooling rate and of annealing time and temperature. Very likely, the observed phase separation is due to the different solubility of the polymer and the dye in the solvent used for film casting. On the other hand, the absence of dye crystals in heated films indicates that the investigated dyes are indeed soluble within the polymer matrix because of the favourable interactions between azobenzene residues and polar VAc repeating units. Accordingly, a large content of apolar ethylene residues limits the DEAz solubility in EVAc matrices.

3.3. Thermal properties

The thermal stability of the investigated dyes, polymers, and DEAz-polymer host–guest systems was evaluated by thermal gravimetry analysis (TGA) under nitrogen atmosphere. All analyzed samples presented less than 5% mass residue (MR_{600}) at 600 °C (Table 3). DEAz and DHAz decomposed in a single step. Their onset (T_d) and peak (T_{d1}) decomposition temperatures are 195 and 313 °C (DEAz) and 303 and 392 °C, respectively. Although it is not easy to explain the observed differences, these data demonstrate that both dyes can be melt processed with most commodity plastics. The thermal degradation of vinyl acetate

Table 3
Thermal gravimetry analysis (TGA) of the investigated dyes, polymers, and DEAz-polymer host–guest systems

Sample	Polymer	Dye (wt%)	T_d (°C)	T_{d1} (°C)	ΔW_1 (wt%)	T_{d2} (°C)	ΔW_2 (wt%)	MR_{600} (wt%)
DEAz	–	100	195	313	98.7	–	–	1.3
DHAz	–	100	303	392	99.8	–	–	0.2
sE09	EVAc09	0	338	368	7.5	478	92.3	0.2
sE25	EVAc25	0	320	361	18.7	478	80.4	0.9
sE25e3	EVAc25	3	301	358	20.7	474	79.0	0.3
sE40	EVAc40	0	313	358	29.5	470	70.3	0.2
sE40e3	EVAc40	3	303	361	30.9	478	68.7	0.4
SPV	PVAc	0	281	350	71.4	462	23.7	4.9
sPVe3	PVAc	3	285	350	71.5	462	24.4	4.1

T_d is the onset decomposition temperature, evaluated as 1% weight loss; T_{d1} and T_{d2} are the temperatures at the inflection point of the first and second decomposition steps; ΔW_1 and ΔW_2 are the weight losses of the first and second decomposition steps; MR_{600} is the mass residue at 600 °C.

Table 4
Glass transition (T_g) and melting (T_m) temperatures of polymer–dye films prepared by solution casting (SC) and by melt processing (MP)

Polymer	Azo dye		Film type	T_{g1} (°C)	T_{g2} (°C)	T_m (°C)
	(Type)	(%)				
PVAc	–	–	SC	–	41.5	–
	DEAz	3.0	SC	–	37.2	–
	DEAz	0.1	SC	–	33.8	–
	DHAz	0.3	SC	–	30.7	–
	DHAz	0.1	SC	–	32.2	–
EVAc40	–	–	SC	−32.7	46.1	47
	DEAz	3.0	SC	−30.3	41.7	49
	DEAz	0.1	SC	−27.0	37.8	47
	DHAz	0.3	SC	−30.3	34.6	48
	DHAz	0.1	SC	−31.0	37.8	49
EVAc25	–	–	SC	−31.2	–	75
	DEAz	3.0	SC	−23.5	63.7	75
	DEAz	0.1	SC	−20.2	–	73
	DHAz	0.3	SC	−20.2	–	74
	DHAz	0.1	SC	−25.4	–	74
PVAc	–	–	MP	–	41.9	–
	DEAz	0.1	MP	–	42.9	–
	DHAz	0.1	MP	–	42.8	–
EVAc40	–	–	MP	−30.5	33.3	46
	DEAz	0.1	MP	−29.3	34.5	48
	DHAz	0.1	MP	−31.3	35.5	48
EVAc25	–	–	MP	−26.4	–	75
	DEAz	0.1	MP	−31.2	–	75
	DHAz	0.1	MP	−31.1	–	75
EVAc14	–	–	MP	−23.1	–	92
	DEAz	0.1	MP	−27.2	–	92
	DHAz	0.1	MP	−28.2	–	92
EVAc9	–	–	MP	−22.4	29.4	99
	DEAz	0.1	MP	−23.2	–	99
	DHAz	0.1	MP	−26.2	–	98

homopolymer and copolymers occurred in two-steps. The maximum degradation rates moved from 368 to 350 °C, and from 478 to 462 °C on increasing the vinyl acetate content from 9 to 100%. Correspondingly, the relevant weight losses increased from 7.5 to 71.4% and decreased from 92.3 to 23.7%. As expected, the presence of 3% DEAz did not cause any significant variation of the position and relative extent of the two degradation processes.

The thermal behavior of dyes, polymers, and host–guest systems was investigated by differential scanning calorimetry (DSC). On heating, DEAz and DHAz showed an endothermal transition, attributable to the melting of the dye, at 146 and 34 °C with ΔH_m 144 and 47 J/g, respectively. Data relevant to the second heating scan of the prepared host–guest systems are summarized in Table 4. Depending on polymer composition, the DSC traces presented glass transitions at about −30 °C (T_{g1}, ethylene segments) and/or 40 °C (T_{g2}, vinyl acetate sequences) [31]. EVAc films showed also an endothermal transition in the 47–99 °C range that was attributed to the melting of crystalline ethylene segments. In no case, an endothermal transition attributable to the melting of the guest dye was observed, as expected because of the small dye content. However, the melting of DEAz crystals in cast films was observed by hot stage microscopy at a temperature slightly lower than that of the pure dye.

Both dyes caused the decrease of cast film T_{g2}, in agreement with the occurrence of interactions between the guest dye and the vinyl acetate polymer component. This effect was larger at lower DEAz contents, possibly because of the competition between plasticizing and strengthening effects by the dissolved dye and dye crystals, respectively. On the contrary, the T_{g2} decrease was more pronounced at higher DHAz contents, suggesting that the dye was acting only as a plasticizer. Indeed, POM analysis showed that DHAz is actually soluble in VAc-rich polymers. Both azoaromatic guests caused a small increase of the glass transition (T_{g1}) relevant to the ethylenic polymer component, suggesting that the dyes favoured the polymer crystallization. On the other hand, the melt processed host–guest systems presented glass transitions at temperature always slightly larger than that of the corresponding host polymer (Table 4). Apparently, the dye exerted a filler effect, although no dye crystal was detected at the optical microscope. It is possible that the high viscosity of the molten systems inhibited the formation of homogeneous polymer–dye host–guest systems. Another more likely explanation is that the interactions among VAc units and

Table 5
UV–vis characteristics of the prepared azo dyes

Sample	λ_1 (nm)	ε_1 (l mol^{-1} cm^{-1})	λ_2 (nm)	ε_2 (l mol^{-1} cm^{-1})
DEAz	330	30,600	460	695
DHAz	330	33,900	461	730

In chloroform solution at 25 °C.

rigid DEAz molecules can act as weak physical crosslinks giving rise to a limited stiffening of polymer backbone. On the other hand, the purified polymer obtained after repeated precipitation of the dye–polymer blends did not display any UV–vis absorption. This result ruled out the polymer stiffening because of thermally induced transesterification reactions between VAc units and azo-dyes. The reported data demonstrate that the preparation method had a clear influence on the dispersion characteristics.

3.4. UV–vis absorption spectra

All polymer films were characterized by UV–vis spectroscopy in the 250–700 nm spectral range. For comparison, the spectra of the synthesized dyes were also recorded (Table 5). The spectra of DEAz and DHAz presented a strong absorption band at 330 nm and a weaker band at 460 nm, attributable to $\pi \rightarrow \pi^*$ and $n \rightarrow \pi^*$ electronic transitions [30], respectively. The UV spectra of cast films containing at least 0.3% DEAz presented a significant scattering component that was attributed to the presence of dye crystals. On the other hand, films containing 0.1% DEAz or 0.1–03% DHAz did not display any scattering. This behavior confirmed the absence of dye crystals. Table 6 summarizes data relevant to the absorption characteristics of host–guest films. When appropriate, the reported absorbance data were corrected for the observed light scattering. Independent of the preparation method, no significant shift of either $\pi \rightarrow \pi^*$ or $n \rightarrow \pi^*$ absorption bands was observed. In most cases, the longer wavelength absorption band was not easily identified, because of its low intensity and of light scattering by the heterogeneous films. Moreover, no direct proportionality among absorbance, thickness, and dye content of the films was observed. This

Table 6
UV–vis characteristics of host–guest films

Film type	Host polymer	Guest dye		Thickness (μm)	A_1	λ_1 (nm)	A_2	λ_2 (nm)
		(Type)	(%)					
SC	PVAc	DEAz	0.1	70	0.94	330	–	–
SC	PVAc	DEAz	0.2	98	2.00	330	–	–
SC	PVAc	DEAz	0.3	110	1.37	330	–	–
SC	PVAc	DHAz	0.1	110	0.71	330	0.04	460
SC	PVAc	DHAz	0.2	110	0.44	330	–	–
SC	PVAc	DHAz	0.3	60	1.44	331	0.04	455
SC	EVAc40	DEAz	0.1	115	1.74	331	0.04	464
SC	EVAc40	DEAz	0.2	65	0.99	331	–	–
SC	EVAc40	DEAz	0.3	88	1.80	331	0.05	465
SC	EVAc40	DEAz	0.3	130	3.00	329	0.09	460
SC	EVAc40	DHAz	0.1	120	1.72	331	0.08	460
SC	EVAc40	DHAz	0.2	95	1.48	331	0.09	460
SC	EVAc40	DHAz	0.3	135	2.41	331	0.09	458
SC	EVAc25	DEAz	0.1	125	1.21	332	–	–
SC	EVAc25	DEAz	0.2	105	2.34	331	0.01	463
SC	EVAc25	DEAz	0.3	49	0.65	331	–	–
SC	EVAc25	DEAz	0.3	100	0.92	331	–	–
SC	EVAc25	DHAz	0.1	85	1.19	332	0.05	461
SC	EVAc25	DHAz	0.2	130	2.22	331	0.08	461
SC	EVAc25	DHAz	0.3	125	2.79	332	0.07	461
MP	PVAc	DEAz	0.1	45	0.55	332	–	–
MP	PVAc	DHAz	0.1	15	0.55	332	–	–
MP	EVAc40	DEAz	0.1	40	0.38	332	–	–
MP	EVAc40	DHAz	0.1	40	0.24	332	–	–
MP	EVAc25	DEAz	0.1	40	0.54	332	–	–
MP	EVAc25	DHAz	0.1	45	0.31	332	–	–
MP	EVAc14	DEAz	0.1	55	0.54	332	–	–
MP	EVAc14	DHAz	0.1	15	0.25	332	–	–
MP	EVAc9	DEAz	0.1	60	0.58	332	–	–
MP	EVAc9	DHAz	0.1	60	0.26	332	–	–

In chloroform solution at 25 °C; SC, solution cast films; MP, melt processed film. A_1 and A_2 are the abosrbances at λ_1 and λ_2, respectively.

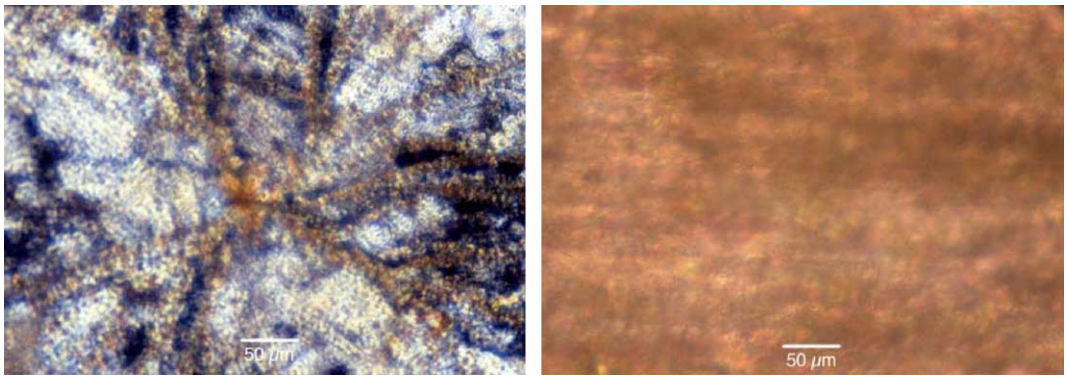

Fig. 4. Polarized light micrographs of EVAc25 cast film containing 1% DEAz before (left) and after 8-fold stretching (right).

Table 7
Optical properties of EVAc/DEAz and EVAc/DHAz films

Film		Dye		SR	*R*	*S*	*PE*	T_{sp}
Sample	Type	Type	(%)					
sE25e01	SC	DEAz	0.1	4	1.3	0.08	0.09	0.46
sE25e01	SC	DEAz	0.1	8	2.2	0.29	0.20	0.59
mE25e01	MP	DEAz	0.1	4	1.1	0.02	0.02	0.50
mE25e01	MP	DEAz	0.1	8	1.2	0.07	0.03	0.72
sE25h01	SC	DHAz	0.1	4	0.80	0.07	0.13	0.32
sE25h01	SC	DHAz	0.1	8	0.91	0.03	0.01	0.79
mE25h01	MP	DHAz	0.1	4	0.82	0.06	0.02	0.79
mE25h01	MP	DHAz	0.1	8	1.1	0.04	0.01	0.80
sE25e03	SC	DEAz	0.3	4	0.42	0.24	0.38	0.41
sE25e03	SC	DEAz	0.3	8	0.50	0.20	0.14	0.67
sE25h03	SC	DHAz	0.3	4	0.43	0.24	0.50	0.29
sE25h03	SC	DHAz	0.3	8	0.34	0.28	0.78	0.19
sE25e1	SC	DEAz	1.0	8	0.31	0.30	0.58	0.35
sE25e2	SC	DEAz	2.0	8	0.17	0.38	0.66	0.44
sE25e3	SC	DEAz	3.0	8	0.07	0.45	0.97	0.37

SC, by solution casting; MP, by melt processing; SR, stretch ratio; *R*, dichroic ratio; *S*, order parameter; *PE*, polarization efficiency; T_{sp}, single piece transmittance.

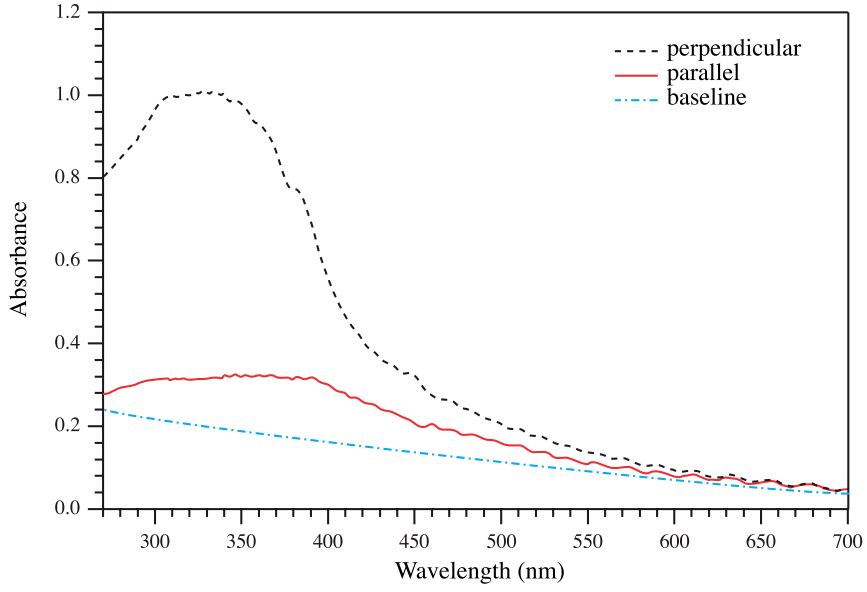

Fig. 5. UV–vis spectra of EVAc25 cast film containing 2% DEAz (Sample sE25e2) recorded with polarized light parallel and perpendicular to the film stretching direction.

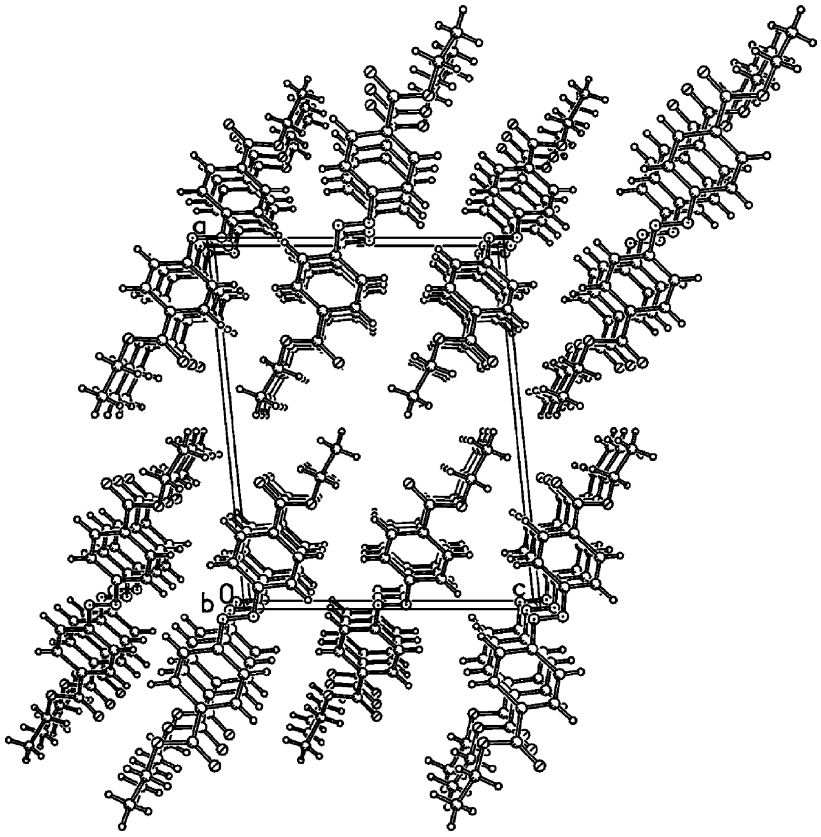

Fig. 6. Crystal structure of *trans*-4,4′-dicarboxyethylazobenzene (DEAz).

result can be attributed to the film heterogeneity as well as to the presence of dye crystals.

3.5. Optical devices

Films obtained by casting and by melt processing of host–guest systems were manually stretched 3–8 times their original length by an hot plate heated at 40 °C. Observation by polarized optical microscopy evidenced the anisotropy of stretched films containing 1–3% DEAz (Fig. 4). Very likely, the drawing process caused the disruption of random aggregates of dye crystals; the resulting needle-like crystals were oriented along the stretching direction.

The UV–vis spectra of stretched films were recorded by a double beam spectrometer equipped with linear polarizers. Measurements were performed by setting the polarizer parallel ($\delta=0°$), diagonal ($\delta=45°$), and perpendicular ($\delta=90°$) to the film stretching direction. The dichroic ratio $R=A_{||}/A_{\perp}$, the order parameter $S=|(R-1)|/(R+2)$, the polarization efficiency $EP=|(T_{||}-T_{\perp})|/(T_{||}+T_{\perp})$, and the single piece transmittance (T_{sp}) are characteristics parameters of polymer film polarizers. The above parameters were evaluated from the maximum absorbance recorded with polarized light parallel ($A_{||}$) and perpendicular ($A_{\perp}$) to the film stretching direction and from the corresponding $T_{||}$ and $T_{\perp}$ transmittance values. In all cases, the recorded absorbance was corrected with a scattering baseline (Fig. 5).

The dichroic ratio R was close to one for films containing 0.1% of DEAz or DHAz, independently of the method of film preparation and extent of stretching (Table 7). Ostensibly, the stretching process did not affect much the orientation of dye molecules. As expected, R was in several cases larger than one, indicating that chromophores aligned along the stretching direction. The dichroic ratio R appreciably decreased and the order parameter S increased, respectively, on increasing the dye content. In any case, an increase of the stretch ratio from 4 to 8 did not substantially affect the induced orientation. Rather surprisingly, the dichroic ratio of all samples containing more than 0.1% dye was appreciably lower than one; that is the absorbance ($A_{\perp}$) of the spectrum recorded with polarized light perpendicular to the stretching direction was larger than that ($A_{||}$) recorded with parallel polarized light. Apparently, the long axis of dye molecules was oriented perpendicularly to the stretching direction. In order to clarify this point, the crystal structure of DEAz was investigated. The X-ray diffraction pattern [32] indicated that the aromatic chromophores were placed almost perpendicularly to the long axis of the needle-like dye crystals (Fig. 6). It seems, therefore reasonable that the film stretching induced a parallel alignment of crystals and hence perpendicular orientation of dye molecules.

The reported behavior clearly shows that the stretching process does not efficiently orient isolated dye molecules. Only host–guest systems constituted by polymer dispersions

of dye micro crystals are effectively oriented, although the dye molecules are aligned perpendicularly to the stretching direction because of the peculiar crystal structure. In this case, the polarization efficiency reaches rather large values that could be exploited for practical applications. Indeed, polarizers for optical displays must present a single piece transmittance larger than 0.35 and a polarization efficiency larger than 0.95. On the other hand, polarization efficiency larger than 0.7 can be sufficient for less demanding applications, such as sun glasses. Interestingly, the film polarization efficiency and hence dye orientation remained almost unchanged for over 1 year.

4. Conclusion

Polymeric host–guest systems can be easily prepared starting from polymers containing vinyl acetate units and two 4,4′-azobenzene diesters containing linear (DEAz) and branched (DHAz) alkyl ester chains. Homogeneous DEAz dispersions can be obtained by solution casting only at dye contents lower than 0.3%, whereas at higher concentration the dye forms phase-separated microcrystals. This behavior was not observed in the case of DHAz, very likely because of the presence of branched alkyl chain that effectively inhibits the crystallization process. At very low dye content, films formed by solution casting or by melt processing have comparable properties, although the latter technique should be preferred because of economic and environmental considerations. Of course, the polymer matrix polarity can significantly affects the dye–polymer compatibility.

Some of host–guest dye–polymer systems afforded films endowed of interesting light polarization efficiency that could be exploited in the production of polymeric polarizers.

Acknowledgements

The authors are grateful to Prof. F. Marchetti (University of Pisa) for X-ray scattering measurements and to Dr A. Pucci and Dr P. Malvadi (University of Pisa) for assistance in light polarization experiments.

References

[1] Delaire JA, Nakatani K. Chem Rev 2000;100:1817.
[2] Xie S, Natanshon A, Rochon P. Chem Rev 1993;5:403.
[3] Eich M, Wehndorff JH. J Opt Soc Am 1990;7:1428.
[4] Ho M, Natansohn A, Rochon P. Macromolecules 1994;27:1885.
[5] Perteson J, Natansohn A, Rochon P. Appl Phys Lett 1996;69:3318.
[6] Xie S, Nathanson A, Rochon P. Macromolecules 1994;27:1885.
[7] Guthrie JT, Dyes, Macromolecular. In: Klingsber A, Muldoon J, editors. Encyclopedia of polymer science and engineering, 2nd ed. New York: Wiley-Interscience; 1996, vol 5, pp. 277.
[8] Brear P, Guthrie JT. Polym Photochem 1982;2:65.
[9] Bellobono IR, Tolusso F, Selli E, Calgari S, Berlin A. J Appl Polym Sci 1981;26:619.
[10] Wang P, Leslie TM, Wang S, Kowel ST. Chem Mater 1995;7:185.
[11] Boutevin B, Granier-Azema D, Rousseau A, Bose D, Guilbert M, Foll F. Polym Bull 1995;34:309.
[12] Kim N. Macromol Symp 1996;101:235.
[13] Andruzzi L, Altomare A, Ciardelli F, Solaro R, Hvilsted S, Ramanujam PS. Macromolecules 1999;32:448.
[14] Mita I, Horie K, Hirao K. Macromolecules 1989;22:558–63.
[15] Uznansky P, Kryszewski M, Thulstrup W. Eur Polym J 1991;27:41.
[16] Beltrame PL, Beltrame E, Castelli A, Tantardini GF. J Appl Polym Sci 1993;49:2235.
[17] Torodov T, Nikolova L, Tomova N. Appl Opt 1984;23:4309.
[18] Advincula RC, Fells E, Park M. Chem Mater 2001;13:2870.
[19] Altomare A, Carlini C, Ciardelli F, Rosato N, Solaro R. J Polym Sci, Polym Chem Ed 1984;22:1267.
[20] Altomare A, Ciardelli F, Lima R, Solaro R. Polym Adv Technol 1991; 2:3.
[21] Angiolini L, Caretti D, Carlini C, Altomare A, Solaro R. J Polym Sci, Part A: Polym Chem 1994;32:1159.
[22] Altomare A, Andruzzi L, Ciardelli F, Gallot B, Solaro R. Polym Int 1998;47:419.
[23] Tirelli N, Suter UW, Altomare A, Solaro R, Ciardelli F, Follonier S, et al. Macromolecules 1998;31:2152.
[24] Tirelli N, Altomare A, Ciardelli F, Solaro R, Follonier S, Bosshard Ch, et al. Polymer 2000;41:415.
[25] Altomare A, Baronti C, Solaro R. Macromol Chem Phys 2002;203: 1584.
[26] Altomare A, Ciardelli F, Faralli G, Solaro R. Macromol Mater Eng 2003;288:679.
[27] Tomlinson ML. J Chem Soc 1946;756.
[28] Jaycox GD. Polymer 1998;39:2598.
[29] Pucci A, Moretto L, Ruggeri G, Ciardelli F, e-Polymers; 2002 no. 015, http:/www.e-polymers.org
[30] Jaffé HH, Orchin M. Theory and application of ultraviolet spectroscopy. New York: Wiley; 1962.
[31] Turi EA. In: Turi EA, editor. Thermal characterization of polymeric materials, 2nd ed, vol 2. New York: Academic Press; 1997. p. 545.
[32] Marchetti F, University of Pisa, Italy, unpublished data.